

# ‘Graft from’ polymerization on colloidal silica particles: elaboration of alkoxyamine grafted surface by in situ trapping of carbon radicals

Rabi Inoubli\*, Sylvie Dagr  ou, Abdel Khoukh, Fran  ois Roby, Jean Peyrelasse, Laurent Billon\*

*Laboratoire de Physico-Chimie des Polym  res, Universit   de Pau et des Pays de l’Adour, BP 1155, F-64013 Pau Cedex, France*

Received 16 November 2004; received in revised form 14 January 2005; accepted 16 January 2005

## Abstract

We report in this paper an original method for the synthesis of polybutylacrylate grafted on silica particles. First, we use the Stober method to synthesize silica particles with a narrow size distribution. An initiator for radical-chain controlled polymerization is then grafted on the silica surface in two steps. Trimethoxysilylpropyl methacrylate (TPM) is first grafted on silica by simple condensation. Then, an alkoxyamine initiator *N-tert-butyl-N-(1-diethylphosphono-2,2-dimethylpropyl)-0,1-methoxycarbonyl ethylhydroxylamine* (MONAMS) reacts with the C=C double bond of the TPM to form the grafted initiator of radical polymerization. The last step is the grafting of butylacrylate. For this, we use living free radical polymerization that allows to control the molecular weight and the polydispersity of the polybutylacrylate chains. We show that this synthesis method makes it possible to obtain a colloidal suspension of silica particles having a mean size of about 88 nm, a weak polydispersity and an important grafting density of polybutylacrylate (PBA).

   2005 Elsevier Ltd. All rights reserved.

**Keywords:** Stober silica synthesis; Polybutylacrylate monolayers; Controlled free radical polymerization

## 1. Introduction

In recent years, an increasing interest has been devoted to the elaboration of inorganic/organic nanocomposites, especially silica/polymer nanocomposites. Understanding the behavior of these composites implies the control of the interactions at the filler/matrix interface, by chemical attachment of polymer chains on the silica surfaces.

Two methods can be used to graft polymer chains on silica particles. The first method is the ‘grafting onto’ method, where end-functionalized polymers react with the silica surface [1,2]; the main drawback of this method is that it only allows to obtain low grafting densities. The second method is the ‘grafting from’ method, where chains grow up in situ from the surface. The first step of the grafting from process is to synthesize a bifunctional initiator, with one function for the grafting on the surface and another for the

initiation of the polymerization [3–10]. One of the advantages of this method is that the initiator density at the surface can be controlled. The combination of this technique with controlled free radical polymerization also allows to control the structural characteristics of the grafted layer (molecular weight, polydispersity and morphology).

Von Werne and Patten [11] first described the free radical polymerization by Atom Transfer Radical Polymerization (ATRP) of methyl-methacrylate and styrene by using a monoethoxysilane-terminated ATRP initiator to obtain inorganic/organic nanocomposites. There are several other recent examples of the synthesis of hybrid nanocomposites using ATRP in the literature [12,13].

In parallel to ATRP, another technique of ‘Stable-Free Radical Polymerization’ (SFRP) has been developed more recently. Bartholome et al. [7] and Parvole et al. [9] reported the Nitroxide-Mediated Polymerization (NMP) reaction to obtain polystyrene PS and polybutylacrylate PBA grafted on silica nanoparticles, respectively. Moreover, this approach has been used for PBA-grafted silicon wafer in order to create elastomer brushes [8]. Using NMP limits the number of purification steps, as there is no need to eliminate both catalyst (copper) and ligand (amine) that are necessary in the case of ATRP. Furthermore, for the synthesis of

\* Corresponding authors. Tel.: +33 559 407 609; fax: +33 559 407 623.  
E-mail addresses: [rabi.inoubli@univ-pau.fr](mailto:rabi.inoubli@univ-pau.fr) (R. Inoubli), [laurent.billon@univ-pau.fr](mailto:laurent.billon@univ-pau.fr) (L. Billon).

inorganic/organic nanocomposites, the fact that NMP can be performed in bulk allows an in situ synthesis of the composite, with no need to disperse the hairy particles in the polymeric matrix.

The aim of this study is to develop a rapid and easy technique to obtain model hairy particles, with a control on several parameters. We want to obtain a controlled particle size with a narrow size distribution, a grafted layer of controlled length and polydispersity, and the absence of particle aggregates. We have chosen the grafting from method and we present in this paper an original technique of polymerization initiation by in situ trapping of carbon radicals, which avoids long and heavy synthesis of bifunctional initiators.

We initially prepared, by the Stoeber method [14], a colloidal suspension of silica nanoparticles with a narrow size distribution. We performed the polymer grafting in a three-step synthesis. The first step is the grafting of trimethoxysilylpropyl methacrylate (TPM) on silica surface by condensation of silanol functions [15]. The second step consists in trapping an alkoxyamine initiator for living free radical polymerization, on the C=C double bond of TPM. This initiator is the *N-tert-butyl-N-1-diethylphosphono-2,2-dimethylpropyl-0,1-methoxycarbonyl-ethylhydroxylamine* (MONAMS). This is an original method for the grafting of a polymerization initiator on a silica surface, that we called ‘in situ trapping of carbon radicals’. The last step is the effective polymerization of butylacrylate from the silica surface. To have a better control of the molecular weight distribution, a counter radical, *N-tert-butyl-N-1-diethylphosphono-2,2-dimethylpropyl nitroxyl* (SG1), was used. The aim of this paper is to show that this simple method allows to obtain a good grafting density, a controlled chain length of the grafted polymer and finally a preserved colloidal character of the suspension.

## 2. Experimental section

### 2.1. Materials

Toluene (99.5%, Aldrich), absolute ethanol (99.9%, Aldrich), ammonium hydroxide (28% in water, Aldrich), trimethoxysilylpropyl methacrylate (98%, Aldrich), MONAMS (95%) and SG1 (85%) were supplied by Arkema and used as received. Tetraethyl orthosilicate or TEOS (98%, Aldrich) and butylacrylate (99% Aldrich) were distilled under vacuum at room temperature.

### 2.2. Characterization techniques

Thermogravimetric measurements (TGA) were performed on a TA Instrument TGA 2950 at a heating rate of  $10\text{ }^{\circ}\text{C min}^{-1}$  under nitrogen atmosphere (from 50 to  $800\text{ }^{\circ}\text{C}$ ).

The Fourier Transform Infra Red spectra (FTIR) were

recorded using a BRUKER IFS 66 spectrometer at a resolution of  $4\text{ cm}^{-1}$  in absorption mode. Fifty scans were accumulated.

X-ray Photoelectron Spectroscopy (XPS) analyses were performed with a Surface Sciences Instrument spectrometer at room temperature, using a monochromatic and focused (spot diameter of  $600\text{ }\mu\text{m}$ ,  $100\text{ W}$ )  $\text{Al K}_{\alpha}$  radiation ( $1486.6\text{ eV}$ ) under a residual pressure of  $5 \times 10^{-8}\text{ Pa}$ . The hemispherical analyzer worked in constant pass energy mode, with energies of  $50\text{ eV}$  for high resolution spectra and  $150\text{ eV}$  for quantitative analysis.

Size Exclusion Chromatography (SEC) characterization was performed using a 2690 Water System instrument with TetraHydro Furan (THF) as eluent. A calibration curve, established with standard polystyrene, was used for the determination of the polymer molecular weight.

Solid state  $^{13}\text{C}$  and  $^{29}\text{Si}$  NMR spectra were recorded at  $100.6$  and  $79.4\text{ MHz}$  on a Bruker Advance  $400\text{ MHz}$  spectrometer.

A non-commercial dynamic light scattering apparatus DL 135/45, developed at the Institut Français du Pétrole by Didier Frot for concentrated and opaque media, was used to measure particle sizes.

### 2.3. Synthesis

Fig. 1 shows the reaction scheme used in this study, from the silica particles synthesis to the polymer grafting.

#### 2.3.1. Silica particles

The silica particles were synthesized by the Stoeber method [14]. This method allows the preparation of monodisperse silica spheres, with radii ranging from  $10\text{ nm}$  to a few micrometers in a mixture of absolute ethanol, ammonium hydroxide and water, using the so-called ‘sol–gel’ process at low temperature [14–16]. The final particle size depends on the initial concentrations of the

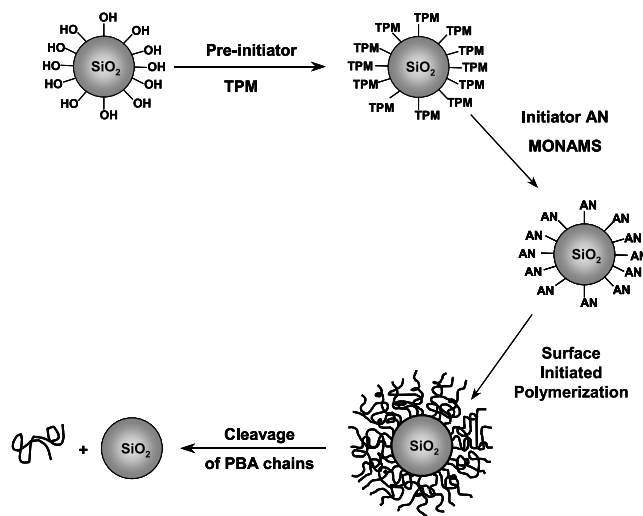


Fig. 1. Scheme of the ‘grafting from’ polymerization.

reactants. For this experiment, 600 ml of absolute ethanol and 32 ml of ammonium hydroxide were mixed. Then 40 ml of TEOS were added quickly in two steps, 20 ml at the beginning of the reaction and 20 ml after 7 h. The reaction mixture was stirred at ambient temperature for 14 h. This procedure allows to synthesize particles with a radius of about 40 nm. The concentration of the suspension obtained is about 3.5 g of silica for 100 ml. These silica bare particles will be named Si in the remaining of the paper.

### 2.3.2. TPM grafting

The grafting of trimethoxysilylpropyl methacrylate (TPM) on the silica surface was obtained by simple condensation of silanol functions as described by Philipse and Vrij [15].

To 300 ml of the silica suspension, 10 ml of TPM (a large excess compared to the concentration of silanol groups on the silica surface) was incorporated and stirred at room temperature during 1h under nitrogen. To favor condensation, 100 ml of the solution were slowly distilled off under vacuum at room temperature. The unreacted TPM was eliminated by a series of centrifugations and dispersions in absolute ethanol. Centrifugation was performed at low speed to avoid aggregation of silica particles. The centrifugation acceleration should be lower than 250g ( $g=9.8 \text{ m/s}^2$ ). Here the protocol is a centrifugation at 3000 rpm during 15 h at 5 °C, followed by washing in absolute ethanol during 10 h under nitrogen. This step has to be repeated 5 times to have a complete purification, which

was checked by UV spectroscopy. The result of this step of the synthesis is a colloidal dispersion of silica particles with grafted TPM, named SiTPM in the following.

### 2.3.3. MONAMS grafting

Usually, for the grafting from polymerization on inorganic surfaces, one needs to synthesize a bifunctional initiator, synthesized via a many-step organic synthesis process [6–9]. We present here an alternative, simple method of in situ trapping of carbon radicals.

This method relies on the following mechanism: in a polymerization reaction, *N-tert-butyl-N-1-diethylphosphono-2,2-dimethylpropyl-0,1-methoxycarbonyl-ethylhydroxylamine* (MONAMS) decomposes, reacts with a C=C monomer double bond (monomer insertion), and recomposes, keeping the living character of the polymerization. The polymerization degree (Dpn) depends on the monomer/initiator molar ratio  $r$ . If  $r \leq 1$ , the monomer insertion is expected to stop after a single monomer insertion. This can be considered as the creation of a macro initiator rather than a polymerization. Here, the double bond that is inserted is the C=C double bond of grafted TPM. Fig. 2 shows the mechanism of the initiator creation by in situ trapping of carbon radicals.

SiTPM was dispersed in Dimethyl Formamide (DMF) (concentration of about 0.02 g of SiTPM/ml). MONAMS was added and the solution was stirred at room temperature under nitrogen during 15 min. The solution is then heated to the reaction temperature. To control this reaction, 5%

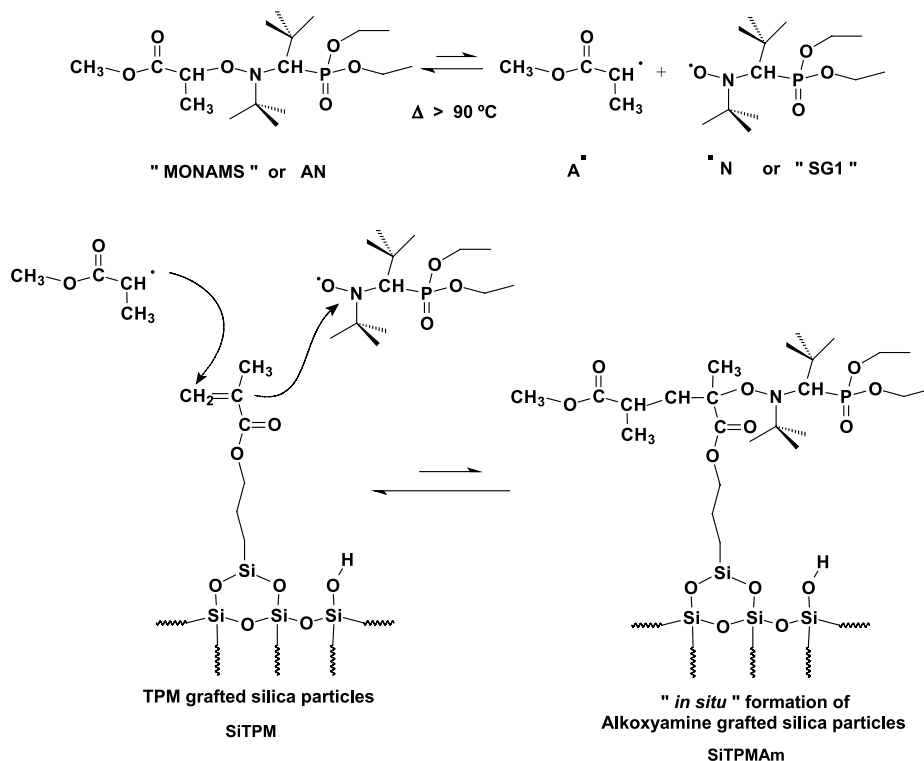


Fig. 2. Initiator (MONAMS) grafting by in situ trapping of carbon radicals.

(in comparison to MONAMS) of SG1 counter-radical were added. Reaction time and temperature have been optimized, and we obtain the sample named SiTPMAm in the following. Unreacted MONAMS and SG1 excess were eliminated by centrifugation and washing in toluene.

#### 2.3.4. Polymerization of butylacrylate

To perform the final polymerization step, 500 mg of SiTPMAm were dispersed in 20 ml of butylacrylate with free MONAMS and an excess of 5% in counter-radical SG1. This system was stirred under nitrogen during 30 min, the reaction of polymerization was performed at 120 °C. The initiator/monomer ratio was adjusted in order to obtain the desired molecular weight [8]. Grafted silica particles were separated from the free polymer by the Prucker and Ruhe procedure [17] with toluene, which is a good solvent for acrylates. Moreover, the acrylic-modified silica particles were carefully extracted several times with toluene and centrifuged, until no precipitate formed when the supernatant solution was added drop wise to an excess of methanol. In parallel, after each cycle of extraction, modified silica passed out of TGA to check the evolution of the weight loss. In this case, the extraction was stopped when the percentage of the weight loss is stable corresponding to 5–10 cycles to remove all non-attached acrylic polymer from substrate.

The polymer layer can be detached from the silica surface, via the initiator ester function, in order to determine the molecular weight of the grafted chains. The cleavage is achieved by acid-catalyzed transesterification with methanol, according to a procedure already reported by Parvole [10] and Prucker [17]. The molecular weights of the non-bonded (degrafted) and grafted polymer were then determined by SEC.

The silica particles grafted with polybutylacrylate

(PBA), obtained at that step, will be named Sig in the remaining of the paper.

### 3. Results and discussion

#### 3.1. Grafting of TPM on silica

##### 3.1.1. Purification of SiTPM

As mentioned in the synthesis part, the elimination of the unreacted free TPM from the grafted silica was carried out by a series of centrifugations and dispersions in absolute ethanol. To control the elimination of free TPM, we measured the UV absorbance of the extracted supernatant after each centrifugation at a wavelength of 203.5 nm which corresponds to the absorbance of TPM. As shown in Fig. 3, a series of five centrifugations and dispersions was necessary to eliminate all the unreacted TPM.

During centrifugation, the aggregation of silica particles can easily happen if the particles are in close contact due to the residual silanol functions of the silica particles or from the partially grafted TPM. For strong accelerations, there will be a complete expulsion of the solvent. As a consequence, silica particles will be in contact and will irreversibly aggregate by condensation of the silanol functions of the silica surface. It is thus important to determine a 'safe' centrifugation procedure after which no aggregates can be detected. Fig. 4 shows the size distributions obtained from dynamic light scattering measurements of the SiTPM samples, after centrifugation at different speeds. Size distribution becomes broader and the maximum moves towards larger radii when the acceleration is increased. From these data, it is unambiguous that high centrifugation acceleration causes an irreversible aggregation of the silica particles.

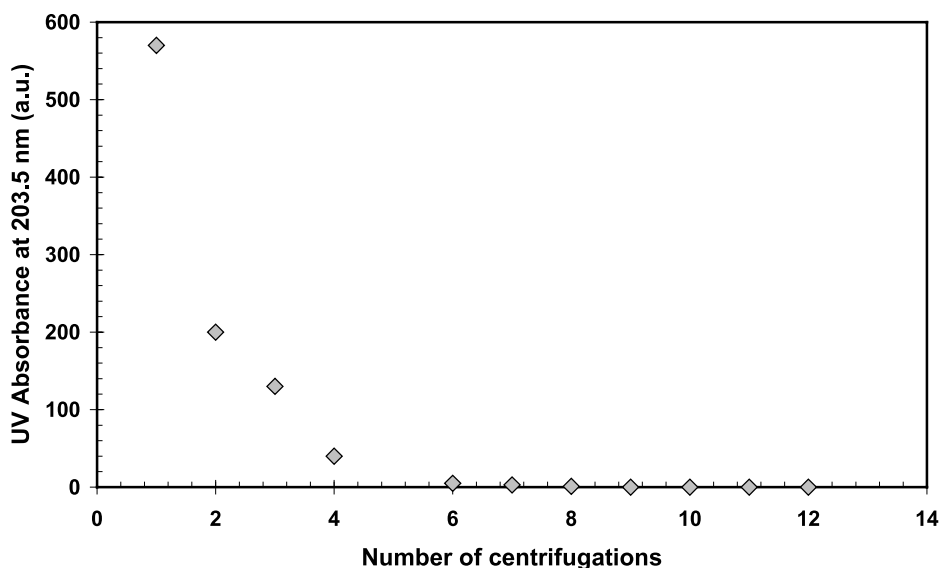


Fig. 3. Variation of the UV absorbance of the supernatant containing free TPM, after centrifugations.

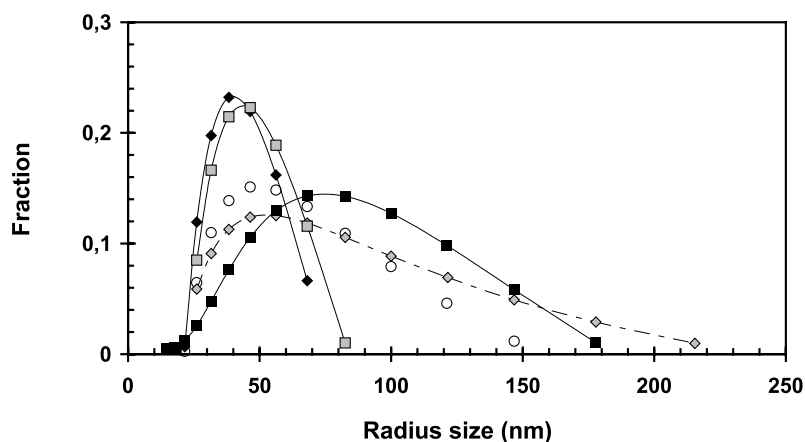


Fig. 4. Size distribution of SiTPM particles as a function of the acceleration applied by centrifugation (◆ pure silica; □ SiTPM centrifuged at 250g during 15 h; ○ SiTPM at 5500g during 6 h; ◇ SiTPM at 10,000g during 1 h; ■ SiTPM at 40,000g during 30 min).

It also appears from Fig. 4 that after an acceleration of 250g, applied during 15 h, the particles do not aggregate, and that the SiTPM suspension is nearly monodisperse, as in the case of pure Si suspension. The mean particle radius increases slightly by about 2 nm after the TPM coating procedure; this increase can be attributed to the hydrodynamic contribution of the TPM layer. These results were confirmed by small angle neutron scattering measurements and will be published in a forthcoming paper. Moreover, similar light scattering results were obtained by Philipse and Vrij [15] on the same system.

### 3.1.2. Characterization of grafted TPM

It was important to verify that TPM was actually grafted on the silica surface. This was achieved by solid state  $^{29}\text{Si}$  and  $^{13}\text{C}$  NMR measurements, by XPS analysis and FTIR measurements.

The  $^{29}\text{Si}$  NMR spectra of pure silica particles (Si) and TPM grafted silica particles (SiTPM) are given in Fig. 5a. Two different components centered at  $-95$  ppm ( $Q_3$ ) and  $-105$  ppm ( $Q_4$ ) can be distinguished on the Si spectrum.

These components can be attributed, respectively, to silicon atoms surrounded by one OH [ $\text{Si}(3\text{OSi}, \text{OH})$ ] or zero OH [ $\text{Si}(4\text{OSi})$ ], respectively. On the SiTPM spectrum, we observed a decrease in the  $Q_3$  component at  $-95$  ppm and the appearance of a new component at  $-50$  ppm, which is characteristic of the T sites [ $\text{Si}-\text{C}$ ]. This component can be attributed to the creation of Si-C bonds by grafting of TPM on the silica surface. These bonds replace the Si-OH bonds, which results in the decrease of the  $Q_3$  component.

The creation of Si-C bonds was confirmed by XPS analysis (Fig. 6). The Si(2p) signal can be decomposed in two peaks at about 103.4 and 101.6 eV, respectively, characteristic of Si-O-Si and Si-O-Si-C links, which is an unambiguous evidence of the presence of a grafted organic layer on the surface of the hybrid inorganic/organic particles.

$^{13}\text{C}$  NMR measurement (Fig. 5b) was used to confirm the presence of TPM on the silica surface. The two vinylic carbons are characterized by peaks at 140 ppm ( $\text{H}_2\text{C}=\text{C}(\text{CH}_3)-$ ) and 127 ppm ( $\text{H}_2\text{C}=\text{C}(\text{CH}_3)-$ ). The peak at 140 ppm is very low intensity due to the long relaxation

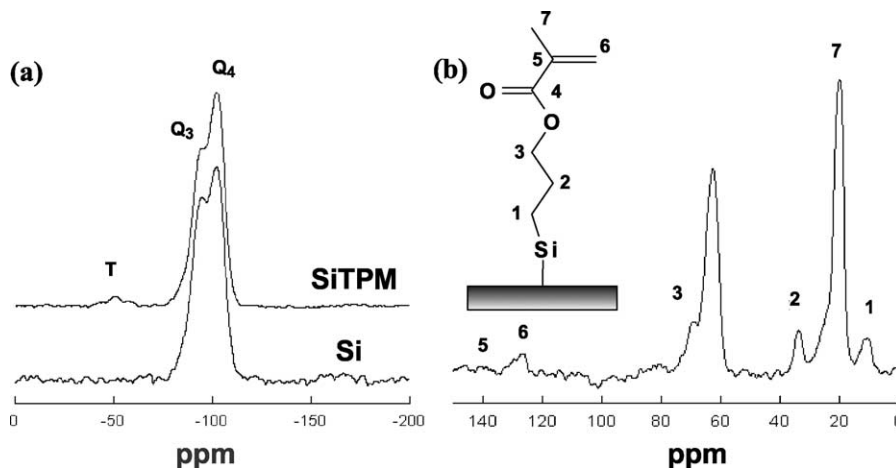


Fig. 5.  $^{29}\text{Si}$  CP/MAS NMR spectra of Si and SiTPM (a) and  $^{13}\text{C}$  CP/MAS NMR spectrum of SiTPM (b).



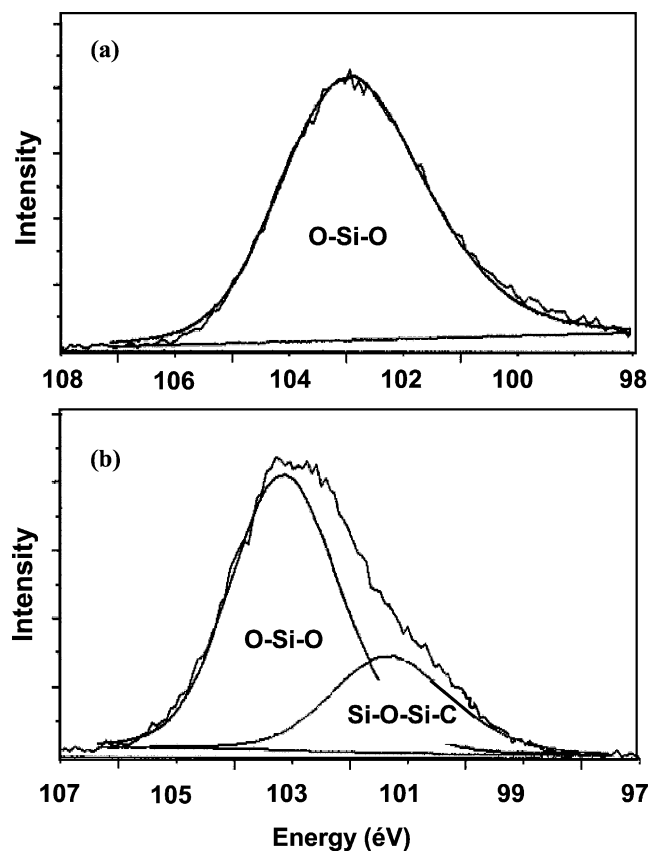


Fig. 6. XPS spectra of Si(2p) signal of pure silica particles (a) and Si(2p) signal of TPM grafted silica particles (SiTPM) (b).

time of quaternary carbon. The three peaks at 10.6 ppm ( $-\text{CH}_2\text{Si}-$ ), 33.8 ppm ( $-\text{CH}_2-\text{CH}_2\text{Si}-$ ) and 69.1 ppm ( $-\text{CH}_2-\text{CH}_2-\text{CH}_2\text{Si}-$ ) have been assigned to the TPM propyl carbons. The methyl group ( $-(\text{CH}_3)\text{C}=\text{}$ ) is characterized by a peak at 20.5 ppm. The  $^{13}\text{C}$  shift value (10.6 ppm) of the ( $-\text{CH}_2\text{Si}-$ ) propyl carbon of TPM near the silicon atom is higher than the chemical shift of the ( $-\text{CH}_2\text{Si}-$ ) propyl carbon of the free TPM (7 ppm). We also have to notice the presence of peaks which are characteristic of unhydrolyzed ethoxy groups from TEOS at 63 ( $-\text{OCH}_2-$ ) and 20.5 ppm ( $-\text{OCH}_2\text{CH}_3$ ). These results confirm the covalent attachment of TPM to the silica surface. Moreover, the absence of a peak at 7 ppm shows the almost complete elimination of the free TPM.

Fig. 7 shows the FTIR spectra of pure silica particles and SiTPM particles. The SiTPM spectrum displays absorption bands at 1720 and 1650  $\text{cm}^{-1}$ . These bands, due to the  $\text{C}=\text{O}$  and  $\text{C}=\text{C}$  bonds, confirm the grafting of TPM. Moreover, the presence of organic part on the silica surface is confirmed by the apparition of peaks characteristic of CH functions.

As a conclusion of this part, characterization of the SiTPM samples by  $^{29}\text{Si}$  and  $^{13}\text{C}$  NMR, XPS and FTIR allows to assert that TPM molecules have been grafted on the silica particles.

### 3.1.3. Determination of the amount of grafted TPM by thermogravimetric analysis

Fig. 8 represents the TGA curves obtained with pure silica (Si) and TPM grafted silica particles SiTPM.

A rather fast weight loss is observed in both cases between 30 and 150 °C. It can be attributed to the solvents that are not completely eliminated after drying at 600 °C under vacuum during 2 days.

Another weight loss appears between 200 and 600 °C. In the case of pure silica, this weight loss may be attributed to the elimination of residues of reactants (ethanol, ammonium hydroxide, water or TEOS) adsorbed on the surface of the silica particles. In the case of the SiTPM samples, this weight loss is rather important, since it includes the weight loss corresponding to the grafted TPM layer. The comparison of the two curves makes it possible to quantify the TPM amount present at the surface. The grafting density of the TPM on the silica surface was determined as follows:

$$\Gamma_{\text{TPM}} = \frac{\frac{W_{\text{SiTPM}}}{100 - W_{\text{SiTPM}}} \times 100 - W_{\text{Si}}}{M \times S_{\text{spe}} \times 100}$$

where  $W_{\text{SiTPM}}$  is the weight loss percent, between 200 and 700 °C, for the SiTPM,  $W_{\text{Si}}$  is the weight loss percent, between 200 and 700 °C, for the pure Si,  $M$  is the molecular weight of the grafted TPM and  $S_{\text{spe}}$  is the specific silica surface area (37  $\text{m}^2/\text{g}$ ).

In order to verify the reproducibility of the condensation of TPM on silica particles surface, three reaction batches have been realized. The TPM grafting density varied from 7.2 to 9.1  $\mu\text{mol}/\text{m}^2$ . The high grafted value obtained here excludes the possibility of a single monolayer. While TPM has three methoxy functions, TPM molecules can condense with one another before condensing on the silica surface, and form multilayers of grafted TPM as described by Philipse and Vrij [15].

### 3.2. Grafting of MONAMS on TPM layer

After the grafting of TPM on the silica surface, we can perform the insertion of MONAMS to create an alkoxyamine initiator by in situ trapping of carbon radicals.

The grafting of MONAMS on attached TPM was performed in dispersed medium, in Dimethyl Formamide (DMF). Thus, to increase the probability of reaction between TPM and MONAMS, it is preferable to introduce a large excess of MONAMS. In this work we have chosen  $[\text{MONAMS}]/[\text{TPM}] = 2$ . The parameters controlling the reaction are the temperature and the reaction time. The following paragraphs are thus devoted to the optimization of these two parameters.

#### 3.2.1. Time effect

We performed the grafting of MOMANS at a temperature of 115 °C with reaction times varying from 5 to 30 min, the other parameters being kept constant. The amount of

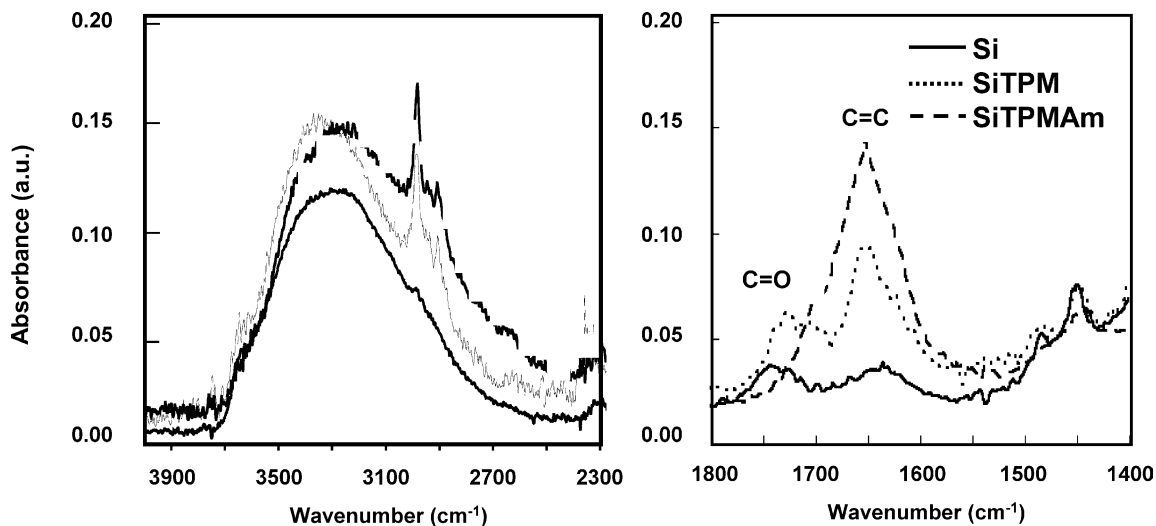


Fig. 7. IR spectra of Si, SiTPM and SiTPMAm particles.

grafted MOMANS was determined by thermogravimetric analysis. The weight loss is that of the sum TPM + MOMANS. Knowing the weight loss of grafted TPM calculated in the previous paragraph, one deduces that of grafted MOMANS. In Table 1 we give for different reaction times the weight loss due to the grafted MOMANS and the calculated grafting density.

It appears that up to a reaction time of 30 min, the grafting efficiency is about constant (about  $1.14 \mu\text{mol}/\text{m}^2$ ). This saturation of MONAMS grafting density can be explained in terms of steric hindrance. For a TPM grafting density of about  $8 \mu\text{mol}/\text{m}^2$ , the distance between two neighboring TPM molecules is estimated to be lower than  $5 \text{ \AA}$  [16]. So when one MONAMS molecule reacts with one TPM C=C bond, the steric hindrance produced is important and prevents the neighboring molecules to react. Another phenomenon can explain this result: there is a possibility of

crosslinking reaction occurring between the adjacent TPM groups on silica during the attachment of MONAMS onto TPM. These results of initiator grafting are in good agreement with the results obtained by several authors using nitroxide [6–9] but it was twice lower than the values given in the literature for ATRP. For example, Von Werne [11] reported a surface coverage of around  $2.4 \mu\text{mol}/\text{m}^2$  for the grafting of a ATRP initiator. Parvole et al. [9] showed that the grafting density of alkoxyamine initiator is lower than that of ATRP initiator, because of the larger steric hindrance of the alkoxyamine.

### 3.2.2. Temperature effect

MONAMS initiating happens between 90 and  $120 \text{ }^\circ\text{C}$  [8]. It is relevant to check the influence of temperature on the MONAMS grafting. SiTPM has been reacted with MONAMS at several temperatures ranging from 85 to

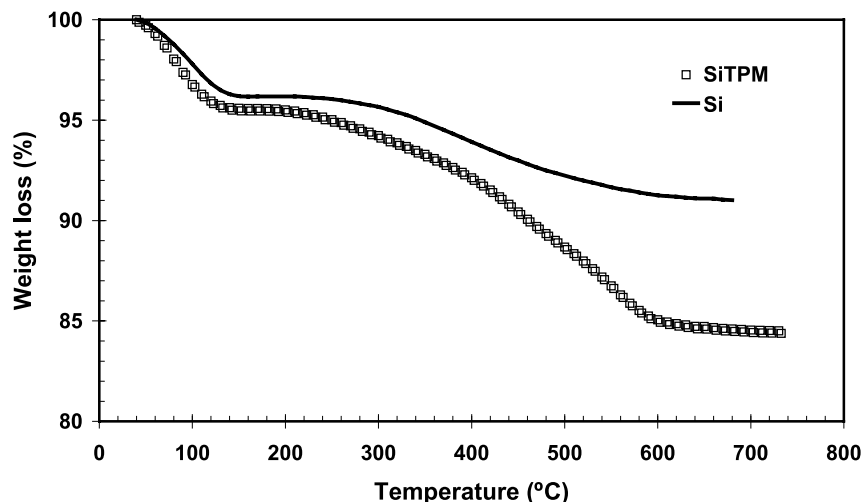


Fig. 8. Thermogravimetric analysis of Si and SiTPM particles.

Table 1  
Variation of MONAMS grafting density with temperature and reaction time

Sample name	Temperature effect				Reaction time effect		
	Am 85	Am 100	Am 115	Am 130	Am 5 mn	Am 15 mn	Am 30 mn
Reaction time (min)	20	20	20	20	5	15	30
Temperature (°C)	85	100	115	130	115	115	115
Weight loss (%) <sup>a</sup>	9.4	10.38	10.40	10.41	10.39	10.42	10.29
Weight loss due to grafted MONAMS (%)	0.35	1.42	1.45	1.42	1.43	1.44	1.29
Density of grafted MONAMS ( $\mu\text{mol}/\text{m}^2$ )	0.27	1.12	1.14	1.12	1.14	1.14	1.02

<sup>a</sup> Weight loss for pure colloidal silica particles Si 5.17% and for TPM modified particles SiTPM 9.08%.

130 °C for a reaction time of 20 min, the other parameters being kept constant. When the reaction temperature is in the cleavage temperature range, Table 1 shows that the reaction temperature has no significant effect on the MONAMS grafting density.

To summarize, the optimal conditions for the ‘in situ’ radicals trapping of MONAMS are a reaction time of 15 min at a temperature of 115 °C with a MONAMS/TPM ratio of 2.

### 3.2.3. Characterization of grafted MONAMS

With Fourier Transform InfraRed spectroscopy (Fig. 7), we have obtained further evidence of the grafting of MONAMS on TPM C=C double bond. The signal of TPM C=C bond, at about  $1640\text{ cm}^{-1}$ , decreases after MONAMS grafting. The C=O bond signal ( $1720\text{ cm}^{-1}$ ) increases at the same time. The C=C bond signal decrease is the consequence of the insertion of TPM in MONAMS and the C=O signal increase is the consequence of the MONAMS presence. To confirm this result, an XPS analysis was performed (Fig. 9).

The spectrum of the pure silica (a) shows signals due to the presence of silicon (152 and 103 eV) and oxygen atoms (533 eV). We also see carbon atoms at 285 eV, due to the residual components of the synthesis of the silica particles. On the spectrum of SiTPM (b), the signal of C increases; at the same time, the signal of Si decreases, due to the presence of TPM molecules at the surface. On the SiTPMAm spectrum (c), we can detect at 400 eV a low signal (corresponding to an amount lower than 1%) due to the presence of the nitrogen of MONAMS; the C/O ratio also increases (from 0.17 for the Si ample, to 0.56 for the SiTPMAm sample). These results show an increase of the organic materials at the silica surface, which corresponds to the presence of TPM and MONAMS on the particles surface.

<sup>13</sup>C NMR spectrum of SiTPMAm is presented in Fig. 10. The peaks observed on this spectrum can be attributed to the various carbons of TPM and MONAMS [18], and the

presence of C<sub>6</sub> peak confirms the fact that MONAMS molecules have not reached all TPM C=C bonds.

The spectrum exhibits all characteristic signals of grafted MONAMS: C<sub>18</sub> and C<sub>8</sub> at 21 ppm, C<sub>13</sub> and C<sub>16</sub> at 35 ppm, C<sub>15</sub> at 41 ppm, C<sub>17</sub> and C<sub>12</sub> at 63 ppm; C<sub>14</sub> at 69 ppm and C<sub>10</sub> at 168 ppm. It is very interesting here, to note that there is no characteristic signal of the (–CH–ON–) bond of free MONAMS (at about 77 ppm on the <sup>13</sup>C spectrum of free MONAMS [18]). This absence shows that there are no free MONAMS and is an indication of the MONAMS grafting on TPM.

As a conclusion, characterization of SiTPMAm by FTIR, <sup>13</sup>C NMR and XPS allows to assert that MONAMS molecules have reacted with the TPM C=C double bonds

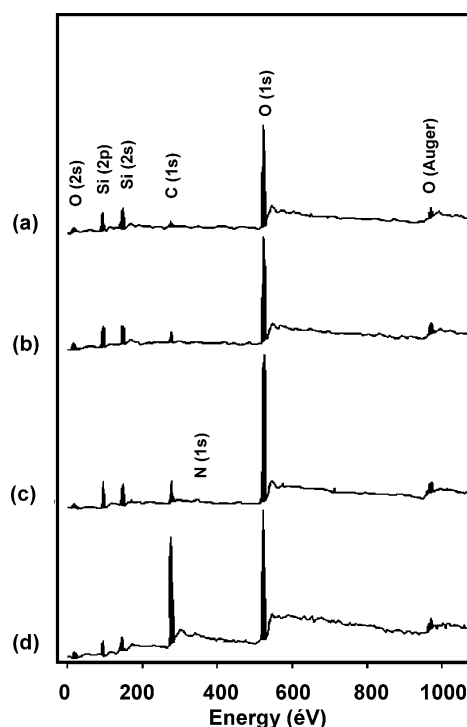


Fig. 9. XPS analysis of (a) Si; (b) SiTPM; (c) SiTPMAm and (d) Sig.



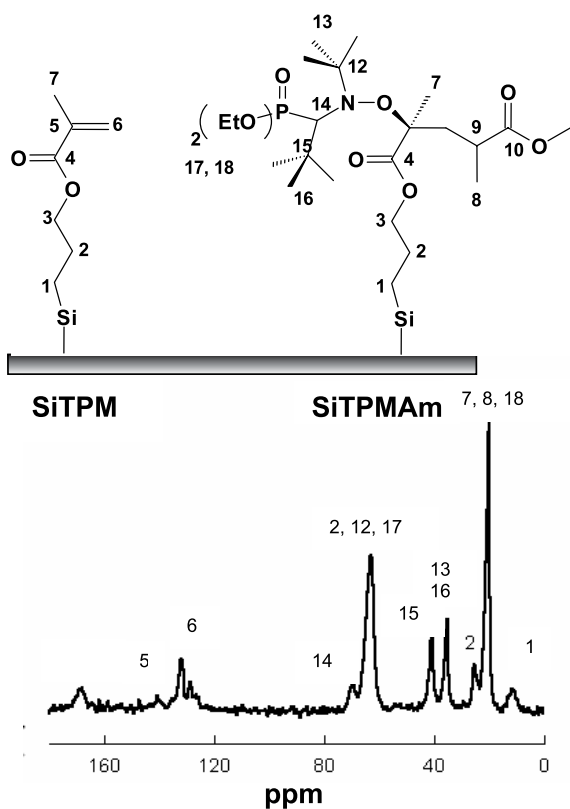


Fig. 10.  $^{13}\text{C}$  NMR spectrum of SiTPMAM.

present on the silica surface. A macroinitiator is thus grafted on the silica surface, and we can perform the grafting from of polybutylacrylate.

### 3.3. Grafting of polybutylacrylate

In this study, the polymerization has not been optimized. The goal was rather to check that this new method could initiate polymerization from the surface. To keep the control of the polymerization, SG1 (Fig. 2) counter radical was added to the system. Parvole [8] shows that with an SG1 excess of 5% compared to the initiator amount, the polymerization control can be kept, which allows to obtain a narrow molecular weight distribution. The polymer layer on the silica surface will then be homogenous.

The experimental polymerization conditions are as follows, monomer/initiator ratio = 500, a reactor temperature of 120 °C with a reaction time of 4h in order to obtain a conversion rate lower than 50% and an expected  $M_n = 30$  kg/mol as described and predicted by Parvole [8].

The results obtained from TGA on these PBA grafted silica particles (Sig) show the presence of organic material, with a weight loss of about 27%. SEC analysis is performed after polymer degrafting, as described in the experimental part. As expected by Parvole work's [8], we obtain a molecular weight of 30,150 g/mol for bulk polymer and 29,500 g/mol for grafted polymer, with a polydispersity index lower than 1.1 in both cases. Moreover, in a previous

study [6,10], we had observed a difference of molecular weight between free and grafted PBA chains. This work was realized with fumed silica particles characterized by a very hairy structure and high porosity. With this type of structure, monomer diffusion has to be limited and thus reduced the kinetic and the molecular weight for a same time of polymerization. By comparison, in the present study the silica particles used are well-defined with a spherical shape and the grafted chains have to grow in the same manner of the free chains with no effect of monomer diffusion on the silica surface.

The XPS analysis (Fig. 9d) confirms these results, as the C/O ratio increases (from 0.56 for the SiTPMAM sample to 2.33 for the Sig sample).

From the TGA results, and from the knowledge of the grafted PBA molecular weight, PBA grafted density was calculated to  $0.22 \mu\text{mol}/\text{m}^2$  (or 0.13 molecule/nm, which corresponds to about 3000 chains/particle). The efficiency of the initiating is about 20%. This results is consistent with other results obtained by nitroxide initiating [7,8]. Other studies [19–22] demonstrated that this grafting density is sufficient to have PBA brushes on the silica surface. To confirm that, we compare the Flory radius ( $R$ ) of the free PBA chains with the average ( $D$ ) distance between grafted sites on the surface. Parvole defined these values in the case of grafted PBA on silica surfaces [8]:

$$R = 0.04M_w$$

$$D = 2(\pi\sigma)^{-0.5}$$

where  $M_w$  is the molecular weight of the PBA chains and  $\sigma$  the grafting density. In our case,  $R = 68 \text{ \AA}$  and  $D = 30 \text{ \AA}$ .  $R$  is thus much greater than  $D$ : the grafted chains stretch to form polymer brushes [20,21].

One can also notice that the PBA grafting density ( $0.22 \mu\text{mol}/\text{m}^2$ ) is much lower than the initiator grafting density ( $1.1 \mu\text{mol}/\text{m}^2$ ). Several studies explain this decrease of the initiator efficiency in terms of ending reactions [8,23] or in terms of temperature promoted degrafting of the initiator or the polymer [24].

### 3.4. Conservation of the colloidal character of the system

After each step, we checked the size distribution of the particles by dynamic light scattering (Fig. 11).

The mean radius of the SiTPMAM particles (45 nm) is slightly larger than that of the pure silica particles (42 nm). This difference can be explained in terms of a hydrodynamic contribution of the TPM and MONAMS layers. The mean radius of the PBA grafted particles (Sig) is about 88 nm. The thickness of the PBA layer can be estimated to be about 45 nm. We can compare this result to the calculations of de Gennes [21] for the thickness of a layer of stretched polymer chains in a good solvent. This calculated value is about 55 nm, in good agreement with our experimental result. The

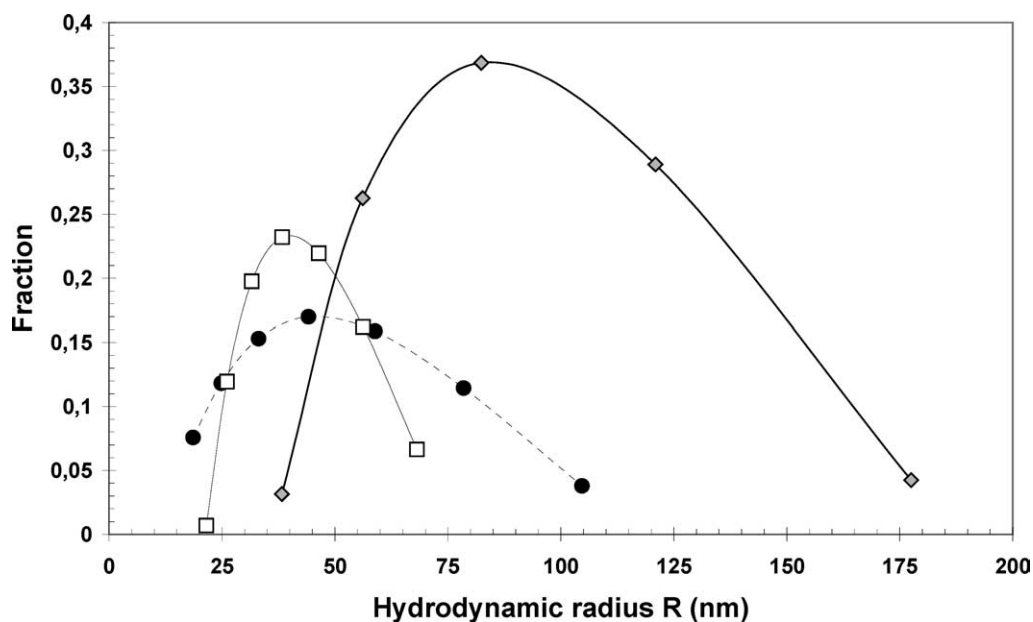


Fig. 11. Size distribution of Si (□), SiTPMAm (●) and Sig (◇) particles.

light scattering results also show that our synthesis method allows us to preserve a narrow size distribution at each step of the process. In other words, aggregation of particles has been avoided.

Fig. 12 is a SEM picture of the PBA grafted silica particles. It was performed on an environmental SEM Electro Scan ESM-E3, with a tungsten filament. It shows that the particles are spherical and that the particle sizes are of the same order of magnitude than that determined by light scattering experiments.

#### 4. Conclusion

Polybutylacrylate grafted silica nanoparticles have been prepared by alkoxyamine-mediated polymerization, using a novel method of in situ trapping of carbon radicals. The reaction scheme presented in Fig. 2 is validated by the characterizations performed by NMR, XPS, FTIR and TGA after each synthesis step. Furthermore, we show that the narrow size distribution of the Stoeber silica particles is

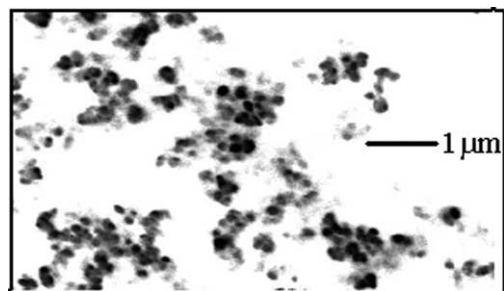


Fig. 12. SEM picture of PBA grafted silica particles.

preserved during grafting from polymerization, so that we can obtain non-aggregated hairy particles at the end of the synthesis process. Finally, using this grafting from technique combined with controlled radical polymerization allows to have a homogeneous polymer layer around the silica particles, with controlled molecular weight and a low polydispersity index.

This original approach is a simple and rapid technique that allows to perform grafting from polymerization by using commercially available reactants only, with no need to synthesize a bifunctional initiator, and with a limited number of synthesis steps. For as far as we know, this is the most simple grafting from technique that allows to obtain a controlled particle size with a narrow size distribution, a grafted layer of controlled length and polydispersity, with no particle aggregates.

Future work will be focused on the control of the polymer grafting density, in order to access several morphologies for the grafted layer. Moreover model filled polymers can be synthesized by this method, with a control on several parameters, such as the particle size and the filler/matrix interface. In order to model the rheological behavior of such a system, the colloidal character is essential, a reason why we pay particular attention to this aspect.

#### Acknowledgements

The authors are indebted to Dr Olivier Guerret, from ARKEMA for supplying MONAMS, and to Dr Claude Guimon for XPS analysis.

## References

- [1] Auroy P, Auvray L, Leger L. *J Colloid Interf Sci* 1992;150:187–94.
- [2] Ebata K, Furkawa K, Matsumoto N. *J Am Chem Soc* 1998;120:7367–8.
- [3] Devaux C. Thesis of ‘Université Claude Bernard, Lyon’; 2001.
- [4] Carrot G, Rutot-Houze D, Pottier A, Degee P, Hilborn J, Dubois P. *Macromolecules* 2002;35:8400–4.
- [5] Chen X, Randall DP, Perruchot C, Watts JF, Patten TE, von Werne T, et al. *J Colloid Interf Sci* 2003;257:56–64.
- [6] Parvole J, Billon L, Montfort JP. *Polym Int* 2002;51:1111–6.
- [7] Bartholome C, Beyou E, Bourgeat-Lami E, Chaumont P, Zydowicz N. *Macromolecules* 2003;36:7946–52.
- [8] Parvole J. Thesis of ‘Université de Pau et des Pays de l’Adour’; 2003.
- [9] Parvole J, Laruelle G, Guimon C, Francois J, Billon L. *Macromol Rapid Commun* 2003;24:1074–8.
- [10] Parvole J, Montfort JP, Billon L. *Macromol Chem Phys* 2004;25:1369–78.
- [11] Von Werne T, Patten TE. *J Am Chem Soc* 2001;123:7497–505.
- [12] Kickelbick G, Holzinger D, Brick C, Trimmel G, Moons E. *Chem Mater* 2002;14:4382–9.
- [13] Pyun J, Kowalewski T, Matyjaszewski K. *Macromol. Rapid Commun* 2003;24:1043–59.
- [14] Stoeber W, Fink A, Bohn E. *J Colloid Interf Sci* 1968;26:62–9.
- [15] Philipse AP, Vrij A. *J Colloid Interf Sci* 1988;128:121–36.
- [16] Bourgeat-Lami E, Lang J. *J Colloid Interf Sci* 1998;197:293–308.
- [17] Prucker O, Ruhe J. *Macromolecules* 1997;31:592–601.
- [18] Couturier JL, Henriët-Bernard C, LeMercier C, Tordo P, Lutz JF. WO 00/49027: US Patent; 2002.
- [19] Aubouy M, Fredrickson GH, Pincus P, Raphaël E. *Macromolecules* 1995;28:2979–81.
- [20] Daoud M, Cotton JP. *J Phys* 1982;43:531–8.
- [21] de Gennes PG. *Macromolecules* 1980;13:1069–75.
- [22] Raphael E, Pincus P, Fredrickson GH. *Macromolecules* 1993;26:1996–2006.
- [23] Husseman M, Malmstrom EE, Hawker CJ. *Macromolecules* 1999;32:1424–31.
- [24] Sedjo RA, Mirous BK, Brittain WJ. *Macromolecules* 2000;33:1492–3.